GEOPHYSICAL RESEARCH LETTERS, VOL. 25, NO.12, PAGES 2045-2048, JUNE 15, 1998

Electron modulation and ion cyclotron waves observed by FAST

J. P. McFadden[1], C. W. Carlson[1], R. E. Ergun[1], C. C. Chaston[1], F. S. Mozer[1], M. Temerin[1], D. M. Klumpar[2], E. G. Shelley[2], W. K. Peterson[2], E. Moebius[3], L. Kistler[3], R. Elphic[4], R. Strangeway[5], C. Cattell[6], R. Pfaff[7]

Abstract. New observations from the FAST satellite demonstrate strong wave-particle interactions between energetic electrons and H+ EMIC waves in inverted-V arcs. The intense waves are shown to occur in strong upward current regions which contain intense downgoing field-aligned electron fluxes. Electrons near the inverted-V spectral peak have large, factor of 2 to 10, coherent flux modulations at or near the wave frequency. The electron modulations are typically centered at about $f_{CH+}/2$, where f_{CH+} is the local H+ cyclotron frequency. The EMIC waves are broadbanded, extending from about $0.3f_{CH+}$ to $0.7f_{CH+}$. These waves also accelerate cold secondary electrons, forming counterstreaming field-aligned electrons at energies up to about 300 eV. In addition, electron modulations at f_{CH+} are observed in the density cavities associated with upgoing ion beams. Intense waves at f_{CH+} are simultaneously detected and shown to have a magnetic component similar to the EMIC waves.

Introduction

Temerin et al. [1986, 1993] developed a model for the interaction between electromagnetic ion cyclotron (EMIC) waves and auroral electrons to account for electron flux modulations observed by sounding rockets. The model postulates that EMIC waves are present below the primary auroral acceleration region, calculates waveforms, and uses a test particle simulation to calculate the resonant interaction between waves and electrons. As EMIC waves propagate down the field line from near resonance ($f \sim f_{CI}$), their parallel phase velocity increases with decreasing altitude and they resonantly interact with both cold secondary electrons and energetic inverted-V electrons. The primary interactions occur at altitudes above the 2-ion hybrid resonance (~2500 km), where the phase velocity of H+ EMIC waves approaches infinity. *Temerin et al.* [1993] showed that observed modulations at ~80 Hz were consistent with resonant interactions with H+ EMIC waves, however no accompanying waves were measured.

This paper presents new observations from the FAST satellite confirming the resonant interaction of the electrons with H+ EMIC waves. The primary interactions are observed between EMIC waves and electrons at altitudes below the potential drop, and at energies near the inverted-V peak energy. We also show that electron modulations and associated waves are present in the ion beam regions, above a portion of the inverted-V potential drop. These modulations are at the local H+ cyclotron frequency, f_{CH+}, whereas the EMIC waves are at lower frequency, closer to $f_{CH+}/2$.

[1]Space Sciences Laboratory, University of California, Berkeley, CA
[2]Lockheed Martin Palo Alto Research Laboratory, Palo Alto, CA
[3]University of New Hampshire, Durham, NH
[4]Los Alamos National Laboratory, Los Alamos, NM
[5]University of California, Los Angeles, CA
[6]University of Minnesota, Minneapolis, MN
[7]Goddard Space Flight Center, Greenbelt, MD

Paper number 98GL00855.
0094-8534/98/98GL-00855$05.00

Instrumentation

The FAST satellite contains two pairs of electrostatic analyzers to measure the high resolution energy/angle spectra of ions (3 eV - 25 keV) and electrons (4 eV - 30 keV) with 78 ms resolution. The spacecraft orientation relative to the magnetic field is such that plasma analyzers measure the full pitch-angle distribution continuously, with time resolution limited only to the analyzer sweep time. These analyzers have deflectors at their entrance apertures to steer their fields-of-view to always include both the parallel and anti-parallel magnetic field line [*Carlson and McFadden*, 1998]. FAST also contains a set of six pairs of electron electrostatic analyzers that measure distribution functions at ms time scales. These analyzers can be configured as spectrographs to perform a 6 energy x 16 pitch-angle distribution measurement with 1.6 ms resolution. For the results described below, the spectrographs are configured for 0.5, 1, 2, 4, 8, and 16 keV energies.

FAST also contains 3-axis electric and magnetic field experiments and a mass spectrometer. The field experiments provide the high resolution waveform data (2 and 8 kHz sampling) shown below. The Time-of-flight Energy-Angle Mass Spectrometer (TEAMS) provides density ratios for H+, O+ and He+ ions [*Moebius et al.*, 1998].

Observations

Figure 1 shows three minutes of FAST particle and wave data taken in inverted-V arcs that contained large electron flux modulations. The data were collected between 3825 and 3675 km altitude at about 21 MLT during a moderately active period (KP=3.7). The vertical lines at 09:11:48 and 09:11:55 mark regions with strong wave particle interactions that will be discussed later. Panels 1 and 2 are ion energy and pitch-angle spectrograms. The pitch-angle spectrograms are displayed from -90° to 270° to reflect the analyzer's 360° field-of-view and to prevent narrow field-aligned beams from appearing on the plot axes. Downgoing fluxes correspond to 0°. Ion beams are seen at 9:11:45 - 9:11:50 and again at 9:14:00 - 9:14:14. Ion beams indicate times when the spacecraft is above a portion of the parallel electric field and in the auroral density cavity. Low-energy ion conics are also seen throughout the region. Analysis of mass spectrometer data for the ion beam at 9:11:47 shows the flux, NV_D, dominated by H+, but with similar beam densities of $N_{H+} \sim N_{O+} \sim 0.35/cm^3$ at ~1 keV.

The electron energy spectrogram, panel 3, shows a series of inverted-V arcs. These arcs occur throughout a transition from a relatively hot (3000 eV) to a cool (500 eV) plasma sheet electron source population (determined by fitting the distribution at energies above the spectral peak). The source population temperature

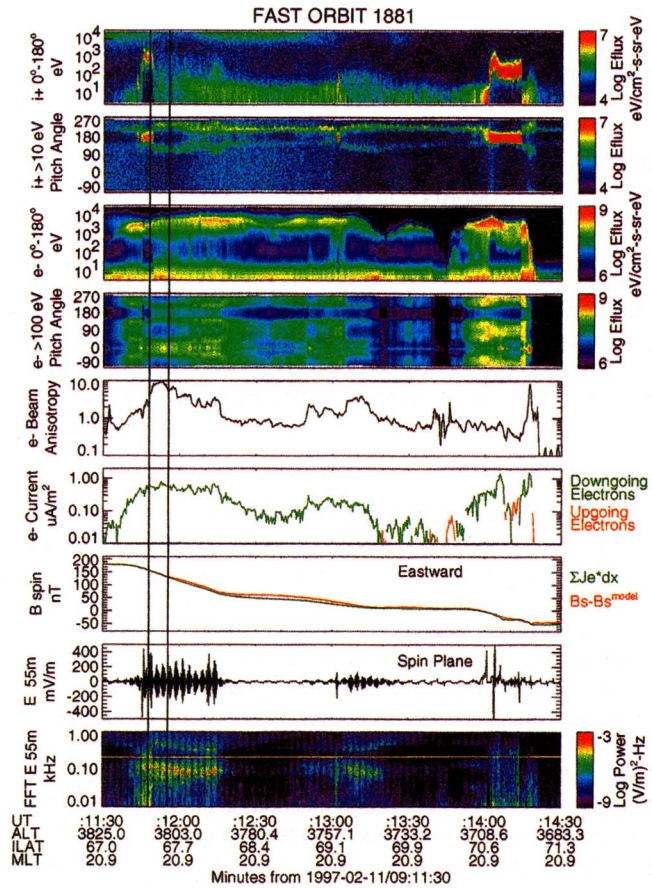

Figure 1. A nightside auroral crossing is shown that contains ion beams (energetic ions in panel 1, with pitch angles near 180° in panel 2) and broad inverted-V arc electron precipitation (panel 3). Intense field-aligned electron fluxes (enhanced flux at 0° pitch angle in panel 4) and electron beam anisotropy greater than 1 (panel 5) are correlated with larger upward currents (panels 6,7), and enhanced waves (panels 8,9). The electron beam anisotropy is defined as the ratio of parallel to perpendicular partial beam densities. Vertical lines correspond to times used for Figures 2-4, which show strong electron flux modulations near the hydrogen cyclotron frequency.

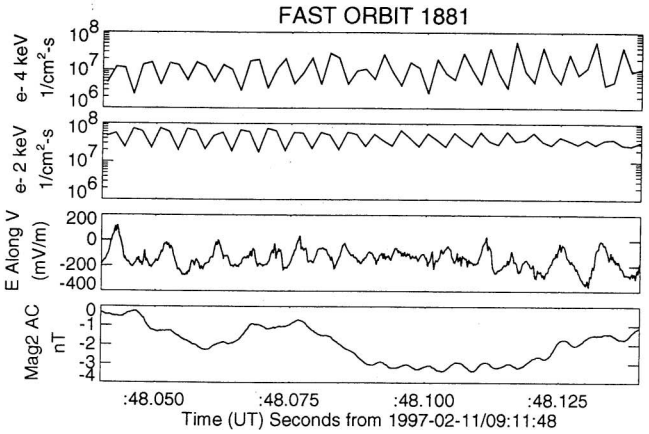

Figure 2. Electrons inside the ion beam region are modulated at the hydrogen cyclotron frequency, f_{CH+}. Electrons with energy above (panel 1) and below (panel 2) the inverted-V spectral peak have modulations that are 180° out of phase, indicating the energy is being modulated and not the total flux. The electric (north) and magnetic (east) fields show a simultaneous f_{CH+} wave.

does not change linearly across the region, but instead drops abruptly from 3000 eV to 500 eV at 9:11:40, then gradually increases to about 2000 eV at 9:12:20, and finally drops off again to about 500 eV at 9:12:50. The electron pitch-angle distribution, panel 4, shows two broad periods with enhanced downgoing field-aligned fluxes: 9:11:45 - 9:12:15, 9:12:50 - 9:13:15. field-aligned fluxes are also seen adjacent to the polar cap (9:14:05 and 9:14:17) in a region with an enhanced trapped population. These periods are easier to identify in panel 5 which shows electron "beam anisotropy" defined as the ratio of parallel to perpendicular partial beam densities, which are partial moments derived from pitch angles 0°-45° and 45°-90°, and from energies within a factor of 2 of the beam energy. The beam anisotropy equals 1 for an isotropic distribution and is greater than 1 for enhanced field-aligned fluxes.

The enhanced field-aligned flux produces a larger electron current as illustrated in panel 6. A comparison of the magnetic deflection estimated from this current (assuming an east-west sheet current) and the spin axis component (eastward positive, perpendicular to $\mathbf{B_0}$ and Vsc) of the magnetic field minus model field, is shown in panel 7. The curves are nearly identical indicating most of the current is carried by the energetic electrons.

The regions with field-aligned electrons and larger currents correspond to regions with intense waves near the local H+ cyclotron frequency, f_{CH+}. Panel 8 is the 2 kHz sampled waveform from a 55 meter spin plane antenna, where the spin plane includes **B**.

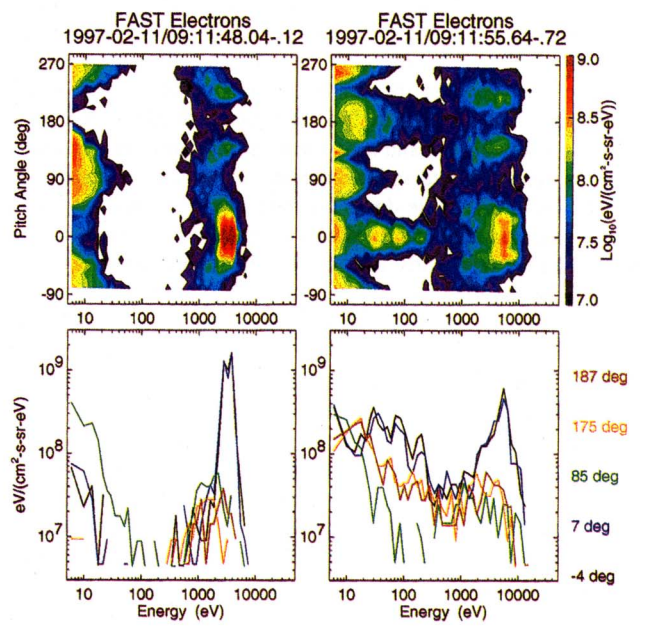

Figure 3. The electron differential energy flux inside the ion beam region (left plots) and outside the ion beam (right plots) show intense downgoing (0° pitch angle) field-aligned fluxes. The left plots correspond to the Figure 2 and contain a double peak due to aliasing between the analyzer sweep and the electron modulation. The right plots correspond to Figure 4 and show broadening due to aliasing between the analyzer sweep and the electron modulation. In the right plots at energies <300 eV, counterstreaming field-aligned fluxes are present with upgoing and downgoing fluxes 180° out of phase suggesting local acceleration of cold secondaries by the waves in Figure 4. Low-energy electrons near 90° and 270° are spacecraft photoelectrons.

Intense waves correlate with regions of enhanced field-aligned flux. Modulation at twice the satellite spin frequency shows that the wave electric field is primarily perpendicular to **B**. Panel 9 shows that the wave power forms two bands, one above and one below f_{CH+} (yellow line at ~0.2 kHz).

Within the ion beams (9:11:45 - 9:11:50; 9:14:00 - 9:14:14), waves at or just above f_{CH+} are observed. Analysis of high resolution data has shown these waves to be narrow-band with additional harmonics. Similar waves measured by the S3-3 satellite were identified as electrostatic ion cyclotron (EIC) waves [*Mozer et al.*, 1977; *Kintner et al.*, 1978], however we refer to them as f_{CH+} waves for reasons discussed below. EMIC waves at about $f_{CH+}/2$ are measured both inside and outside the ion beam region. These waves are more broadbanded, extending from $0.3f_{CH+}$ to $0.7f_{CH+}$. The waves near $2f_{CH+}$ are identified as lower hybrid waves since they have no measurable magnetic component and form the low frequency cutoff of a broader VLF hiss. A saucer signature centered at 9:12 can also be identified in the spectrogram. All of these waves have $E_{\perp}>10E_{||}$ and typical amplitudes from 100-400 mV/m peak-to-peak. The f_{CH+} waves and the EMIC waves also have a magnetic component. *Chaston et al.* [1998] shows the Poynting flux is generally anti-earthward for f_{CH+} waves and earthward for EMIC waves, although large variations occur on ~0.1 second time scales.

The regions containing the intense waves correspond to those with large electron flux modulations. Figure 2 shows a 100 ms stretch of data in the first ion beam (left vertical line in Figure 1) when the f_{CH+} waves were present. The top two panels show the electron count rate from the 4 keV and 2 keV fixed energy detectors, with the electrons modulated at ~f_{CH+}. A ~200 mV/m peak-to-peak 200 Hz wave can be seen in the 8 kHz sampled electric field in panel 3. A ~0.4 nT magnetic signature is simultaneously seen in a perpendicular component of the search coil magnetometer (panel 4). The Poynting flux varies from ~0 to $5x10^{-6}$ W/m^2 (earthward) for the 200 Hz wave.

The two left plots in Figure 3 show the electron distribution corresponding to the fluxes in Figure 2. Both contour and spectra plots of the differential energy flux are shown. The contour plot illustrates the enhanced downgoing field-aligned flux associated with the modulations. Aliasing between the analyzer sweep and the electron modulations show up in the spectra plot as a double peak. An energy shift of the spectral peak, rather than a modulation of the flux, is strongly indicated by panels 1 and 2 of Figure 2. The modulations at 4 keV and 2 keV are 180° out of phase as expected for an ~3 keV spectral peak being shifted up and down in energy by ~1 keV. This wave-electron interaction would appear as parallel heating of the electron beam at lower altitudes where velocity dispersion mixes electrons of different energy.

In contrast, Figure 4 shows a 100 ms interval of data taken outside the ion beam (right vertical line in Figure 1). Panels 1 and 2 show the 16 keV and 8 keV fixed energy channels. The electrons are modulated at ~120 Hz, well below f_{CH+}. Panels 3 and 4 show the electric (~300 mV/m) and magnetic (~1 nT) fields of the corresponding EMIC waves. Note that a phase shift between **E** and **B** occurs across panels indicating a change in polarization of the wave. The Poynting flux changes from $7x10^{-5}$ W/m^2 (earthward) to $-4x10^{-5}$ W/m^2 (anti-earthward) across this interval. Lastly, lower hybrid waves at ~400 Hz can also be identified in panel 3, with no corresponding magnetic signature.

The two right plots in Figure 3 show the electron distribution corresponding to Figure 4. The enhanced field-aligned flux at the inverted-V spectral peak is similar to the flux in the ion beam region (left plots) but with a broader parallel temperature for the electron beam indicating greater parallel heating has taken place.

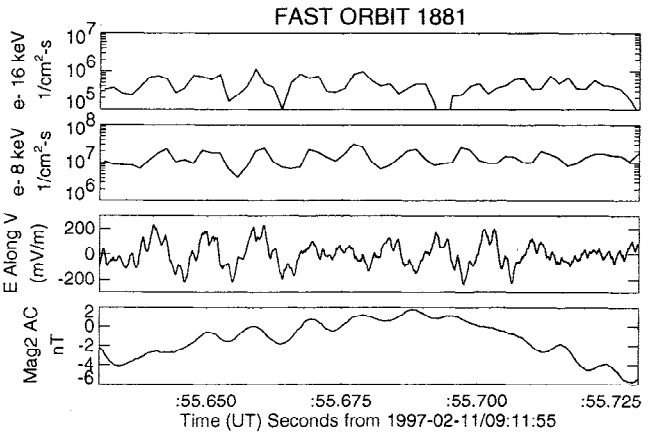

Figure 4. Electrons (panels 1,2) outside the ion beam region are modulated at ~120 Hz, well below the hydrogen cyclotron frequency, f_{CH+}~208 Hz. EMIC waves with the same frequency can be identified in the electric (north) and magnetic (east) fields, along with electrostatic waves at the lower hybrid frequency (~450 Hz).

Aliasing between the analyzer energy sweep and the ~120 Hz modulations can be seen in the spectra plot as shoulders on either side of the primary peak. In addition to the modulated primary electron beam, these distributions also contains a low-energy (<300 eV) counterstreaming field-aligned flux. These field-aligned fluxes are much colder than the primary beam, with perpendicular temperatures of a few eV. The multiple low-energy peaks are formed by aliasing between the analyzer sweep and waves. Measurements on other auroral passes, where the fixed energy detectors were set lower, have shown that these fluxes are indeed modulated. The upgoing and downgoing fluxes are 180° out of phase, suggesting cold secondary electrons are being accelerated both parallel and antiparallel to **B** by the local wave field. Measurement of the pickup of cold secondaries by the H+ EMIC wave confirms the prediction of *Temerin et al.* [1986, 1993] that these waves trap and accelerate secondary electrons producing the observed narrow field-aligned fluxes below the spectral peak in inverted-V arcs.

Discussion

The electron modulation and wave data described above are characteristic of six carefully examined events, and are consistent with the electron modulations of 25 other events identified in the FAST data. Most of these events are from the winter hemisphere (atmosphere in darkness) at high altitude (>3500 km) near 20-24 MLT, during a period where the fixed energy detectors were set to higher energies. The lowest energy inverted-V arc with modulations had a peak energy of about 0.5 keV, and the highest energy arc with modulations had an inverted-V peak energy >30 keV. Low amplitude (<20 mV/m) EMIC waves are often present without observable electron modulation, however these small amplitudes may not produce enough of an energy shift in the electron distribution to be detectable.

The identification of the lower hybrid waves in the region of strong EMIC waves allows a calculation of the density in these regions. Analysis of the nearby ion beams and conics by the TEAMS mass spectrometer shows that the plasma is about 50% oxygen. For $f_{CE}>>f_{PE}$, and $400<f_{LH}<500$, f_{CH+}=208 Hz, and N_{H+}~N_{O+}, one obtains a total density $5/cm^3<N_e<10/cm^3$. This is

about the measured density of the 8 eV to 100 eV atmospheric secondary electrons. The measured hot electron (>100 eV) density, N_{eh}, is dominated by the downgoing beam density, N_b, yielding $0.5N_{eh} \sim N_{eb} \sim 0.2\text{-}0.3/cm^3$, which gives $N_{eb}/N_e \sim 0.03$. This rather large ratio of beam to background plasma may explain the intense EMIC waves. Using equation 11 from *Temerin and Lysak* [1984]: $\gamma/\omega \sim 1.5\ N_{eb}/N_e\ W_b/T_b\ \gamma_0/\omega$, one can estimate EMIC wave growth at higher altitudes before the beam is plateaued. Using the ratio $W_b/T_b \sim 7$ (determined from the data for 9:11:50 - 9:12:15), $\gamma_0/2\pi f_{CH+} \sim 0.1$ for a ~3 keV beam (Lysak, private communication), and $\omega \sim 2\pi f_{CH+}/2$, one obtains $\gamma/\omega \sim 0.06$. This is about the same as the largest estimates of wave growth by *Temerin and Lysak* [1984]. An actual growth rate calculation is beyond the scope of this paper since it would require a simulation that includes the evolution of the electron beam and wave reflections between the 2-ion hybrid resonance altitude and the density cavity associated with the ion beam region. It should be noted that the integrated parallel distribution function shows a broad plateau, with occasional small positive slopes below the spectral peak, suggesting the waves have stabilized the beam.

High resolution waveform data have been examined at the edge of the ion beam (9:11:50) which show that the lower hybrid waves and f_{CH+} waves merge continuously at the boundary. This suggests that the lower hybrid frequency has dropped to just above the ion cyclotron frequency during the ion beam and that the f_{CH+} waves may be lower hybrid waves. However, the f_{CH+} waves have a magnetic component indicating a change in wave mode has occurred. Local measurements by the mass spectrometer within and near the ion beam show $N_{H+} \sim N_{O+}$. Using the higher time resolution ion ESA and correcting for the N_{H+}/N_{O+} density ratio, one obtains an ion density nearly identical to the hot (>100 eV) electron density, with $N_{eh} \sim 0.7/cm^3$ in the ion beam region, suggesting that little or no cold electrons are present. (A future publication will show that the hot plasma dominates the density in the ion beam regions.) Assuming the hot electrons represent the total density, one obtains $f_{LH}/f_{CH+} \sim 1.3$, and the f_{CH+} waves are below f_{LH}, at least for the 9:11:45-9:11:50 event. This combined with the finite magnetic component suggests that cold plasma dispersion is inadequate to explain the observed mode.

It should be noted that the above plasma parameters differ from those determined by *Kintner et al.* [1978] who used the linear instability theory for current driven EIC waves to describe nearly identical f_{CH+} waves. They determined that the plasma was >90% H+, and that the electron temperature was only 3 eV. The above analysis suggests the waves exist in a low density cavity with ~50% O+ and with little or no cold electrons, which precludes the growth of the EIC mode.

Summary

Inverted-V arcs with enhanced field-aligned electron fluxes are shown to contain intense electromagnetic waves with frequencies near the hydrogen cyclotron frequency, f_{CH+}. Large electron flux modulations at the same frequency are observed indicating strong wave-particle interactions are occurring. Inside regions containing ion beams, the largest electron modulations are at or just above f_{CH+} and the associated waves appear to require a hot plasma dispersion analysis to identify the wave mode. Outside the ion beams, the largest electron modulations are near $f_{CH+}/2$ and correlated with H+ EMIC waves. These observations affirm the model by *Temerin et al.* [1993] who predicted resonant interactions between electrons and H+ EMIC waves, and suggests growth rates near the upper limit predicted by *Temerin and Lysak* [1984].

Acknowledgments. The analysis of FAST data was supported by NASA grant NAG5-3596.

References

Carlson, C. W., and J. P. McFadden, Design and applications of imaging plasma instruments, *AGU Monog. Meas. Techn. Space Plasmas*, ed. R. Pfaff, in press, 1998.

Chaston, C. C., et al., Characteristics of electromagnetic proton cyclotron waves along auroral field lines observed by FAST in regions of upward current, *Geophys. Res. Lett.*, in press, 1998.

Kintner, P. M., M. C. Kelley, and F. S. Mozer, Electrostatic hydrogen cyclotron waves near one earth radius altitude in the polar magnetosphere, *Geophys. Res. Lett.*, 5, 139, 1978.

Moebius, E., et al., The 3-D plasma distribution function analyzers with time-of-flight mass discrimination for Cluster, FAST, and Equator-S, *AGU Monog. Meas. Techn. Space Plasmas*, ed. R. Pfaff, in press, 1998.

Mozer, F. S., C. W. Carlson, M. K. Hudson, R. B. Torbert, B. Parady, J. Yatteau, and M. C. Kelley, Observations of paired electrostatic shocks in the polar magnetosphere, *Phys. Rev. Lett.*, 38, 292, 1977.

Temerin, M., and R. L. Lysak, Electromagnetic ion cyclotron mode (elf) waves generated by auroral electron precipitation, *J. Geophys Res.*, 89, 2849, 1984.

Temerin, M., J. McFadden, M. Boehm, C. W. Carlson, and W. Lotko, Production of flickering aurora and field-aligned electron fluxes by electromagnetic ion cyclotron waves, *J. Geophys Res.*, 91, 5769, 1986.

Temerin, M., C. W. Carlson, and J. P. McFadden, The acceleration of electrons by electromagnetic ion cyclotron waves, *Auroral Plasma Dynamics Geophys. Monog.*, 80, 155, 1993.

C. Cattell, University of Minnesota, Minneapolis, MN 55455

R. Elphic, Los Alamos National Lab, Los Alamos, NM 97545

D. M. Klumpar, E. Shelley, and W. K. Peterson, Lockheed Martin Palo Alto Research Laboratory, Palo Alto, CA 94304

J. P. McFadden, C. W. Carlson, R. E. Ergun, F. S. Mozer, M. Temerin, Space Sciences Laboratory, University of California, Berkeley, CA 94720-7450. (e-mail: mcfadden@ssl.berkeley.edu)

E. Moebius, L. Kistler, U. of New Hampshire, Durham, NH 93824

R. Pfaff, Goddard Space Flight Center, Greenbelt, MD 20771

R. Strangeway, University of California, Los Angeles, CA 90095

(Received November 10, 1997; accepted December 16, 1997)